Hyperfine Interaction Measurements on Ceramics: PZT Revisited

Cristiano A. Guarany[a], Eudes B. Araújo[a], Paulo R.J. Silva[b], Henrique Saitovitch[b]
[a]Dept. Física-Química/UNESP - Cx. Postal 31; 15385-000 Ilha Solteira, SP; BRASIL
[b]Centro Brasileiro de Pesquisas Físicas - Rua Dr. Xavier Sigaud, 150; 22290-180 Rio de Janeiro, RJ; BRASIL

1) Abstract: The solid solution of $PbZr_{1-x}Ti_xO_3$, known as lead-zirconate titanate (PZT), was probably one of the most studied ferroelectric materials, especially due to its excellent dielectric, ferroelectric and piezoelectric properties. The highest piezoelectric coefficients of the PZT are found near the morphotropic phase boundary (MPB) ($0.46 \leq x \leq 0.49$), between the tetragonal and rhombohedral regions of the composition-temperature phase diagram. Recently, a new monoclinic phase near the MPB was observed, which can be considered as a "bridge" between PZT's tetragonal and rhombohedral phases. This work is concerned with the study of the structural properties of the ferroelectric PZT (Zr/Ti= 52/48; 53/47) by hyperfine interaction measurements obtained from experiments performed by using the nuclear spectroscopy Time Differential Perturbed Angular Correlation (TDPAC) in a wide temperature range.

2) Introduction: Ferroelectric crystals and ceramics are being studied since many years, enclosing fundamental research concerning their material properties as well as the interests focused on their high potential capabilities for technological applications in devices which could use their remarkable dielectric and piezoelectric prop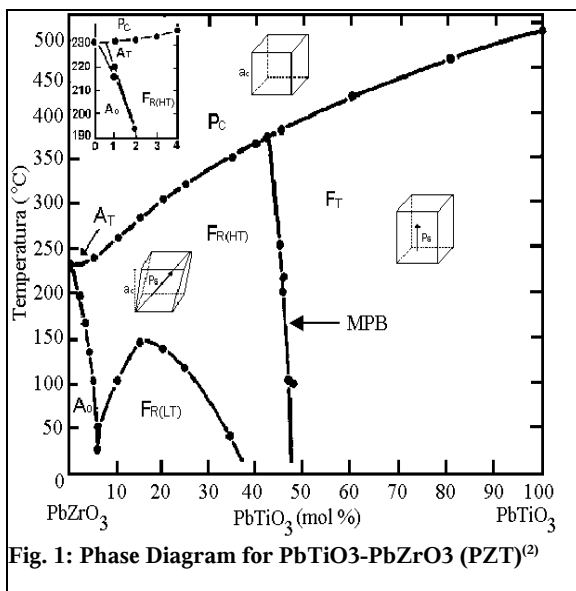erties. Belonging to this context the solid solution system $PbZr_{1-x}Ti_xO_3$, or simply PZT, started to be intensively studied in the '50[1,2]. It's high piezoelectric coefficient are very much requested in the electromechanical industry: radars, hydrophones, ultrasounds, high-voltage sources, micro-positioners etc. It should also be mentioned the variety of PZT's based on the Zr/Ti ratio and their high Curie transition temperature (Tc). A first suggestion for the PZT phase diagram is shown in Fig. 1, which has in its extremities $PbZrO_3$ (lead zirconate) and $PbTiO_3$ (lead titanate). It shows, at the high-temperature paraelectric phase, that PZT has a perovskite cubic structure, with Pb atoms in the vertices of it's cubic unitary cell, Zr/Ti atoms in the center of that cell and atoms of oxygen in the center of the faces of cube forming an octahedral. At low temperatures, PZT assumes a ferroelectric or anti-ferroelectric state, depending on the composition: for a rich Ti composition, PZT displays a tetragonal ferroelectric sructure; while, for a compositions nearer to $PbZrO_3$, PZT assumes a orthorhombic anti-ferroelectric phase. In the region of the diagram where Zr predominates, the crystalline structure is rhombohedric, both at high and low temperatures and, in both cases, ferroelectric.

Fig. 1: Phase Diagram for PbTiO3-PbZrO3 (PZT)[2]

The PZT's highest piezoelectric coefficients are found for compositions near to the so called *morphotropic phase boundary* (MPB)[1]. This MPB region, initially settled for ratios $x \approx 50$ mol % Ti, separates both phases, tetragonal from rhombohedric. As a matter of fact, up to '99 the MPB region was understood as resulting of the coexistence between the tetragonal and rhombohedral phases, and this would explain the well known PZT's improved properties around that region. Nevertheless, theoretical as well as experimental results kept that eventual phases coexistence controversial for several years. Even so, several models favorable to the MPB were proposed, mainly in order to try to explain and justify the high PZT's piezoelectric response in that region[3,4].

Recently the MPB region nature, and consequently the physical properties connected to it's accepted both phases, started to be better understood: using a more appropriate phenomenology, a remarkable improvement was done by conside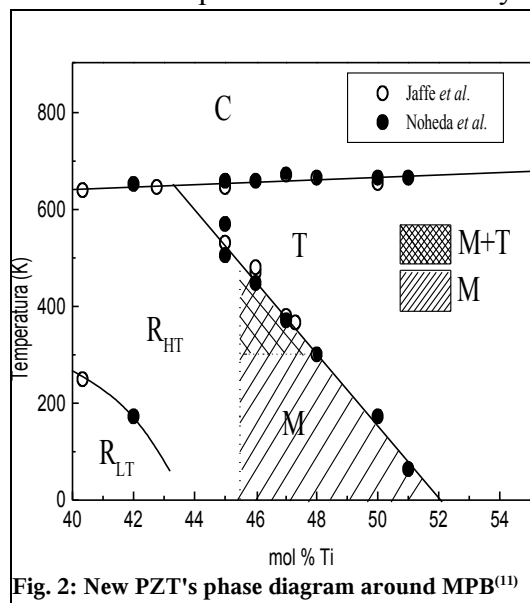ring, for the rhombohedric phase, the piezoelectric response as resulting from a polarization orientation along the [001] direction[5], and not along the [111] direction as it was previously supposed[6]. More recently a new PZT's monoclinic phase was observed near the MPB region. This new phase, exaustively studied by high-resolution X-ray diffratometry (XRD)[7], Raman-spectroscopy[8], dielectric characterizations[9] and electro-mechanical theoretical studies[10] reinforced the arguments concerned with the existence of the [001] polarization orientation cited above. And even more, such studies led to a reformulation of the previous phase diagram with the proposal of a new one around the MPB region[11] (Fig. 2); and also put on evidence that the new monoclinic phase is stable for compositions ratio $.46 \leq x \leq .51$ mol % Ti and is becoming narrower with temperature increase (Fig. 2), which is also responsable for the rhombohedric$\rightarrow$ tetragonal phase transition at x= 0.45.

Fig. 2: New PZT's phase diagram around MPB[11]

Taking into account the PZT compositions around Ti= 0.47, it was proposed[11] a phase transition scheme, temperature dependent, monoclinic$\rightarrow$ monoclinic+tetragonal$\rightarrow$tetragonal, with the suggestion of a probable coexistence of monoclinic and tetragonal phases in the MPB region. In this new context, the monoclinic phase may be considered as a "bridge" between both phases. Nevertheless, the validity limits between the rhombohedric-monoclinic-tetragonal phases remain unclear. Probabely, a fuller understanding of the new monoclinic phase will be the result of the application of several combined techniques in the construction of a new and better consistent PZT phase diagram. With this aim, it's going to be shown in this work hyperfine interaction (HI) measurements results obtained from TDPAC experiments performed on PZT system. This tecnique allows a microscopic study of the charge distributions surrounding isotope-probes incorporated into the samples under study.

3) Experimental Procedure

3.1: Samples Preparation - Samples of PbZr$_{1-x}$Ti$_x$O3 (0.40 < x < 0.52) were obtained through the solid-state reaction from 99.9% pure reagent grade PbO, ZrO$_2$, and TiO$_2$ oxides. The starting powders and distilled water were mixed and milled for 3.5 h for powder homogenization. The mixture was calcined at 850 °C for 2.5 h and then pressed at 400 Mpa, so giving rise to PZT ceramics disks with 10 mm diameter and 5 mm thickness. Finally, the disks were sintered at 1250 °C for 4 h and an excellent homogeneity was obtained. The sintering atmosphere was enriched in PbO vapor by using PbZrO$_3$ powder around the disks inside a covered alumina crucible in order to avoid significant volatilization of PbO.

3.2: TDPAC Spectroscopy and Experimental Set-Up – The expression which describes the time differential modality of the angular correlation function of a nuclear γ-γ cascade, in the particular case of the γ's detection combination at two angles and with it's intermediate state quadrupole moment **Q** interacting with a local electric field gradient (EFG) tensor being therefore modulated by means of the perturbation factor $G_{22}(t)$, is given by[*]:

$$W(\theta,t)=\exp(-t/\tau)\cdot[1+A_{22}G_{22}(t)P(\cos\theta)]$$

The isotope-probe used was ^{181}Ta [^{180}Hf(n,γ)^{181}Hf$\rightarrow$^{181}Ta] produced by neutron irradiation of ^{180}Hf

---

[*]terms of this expression, included the various aspects of TDPAC theory, are described in refs. 12-13

contained in the samples as a Zr impurity. The ^{181}Hf/^{181}Ta concentration was less than ppm. The time spectra were measured with a four BaF$_2$ detector set-up storing twelve coincidence spectra, eight of them at 90º and four at 180º.

4) Results and Discussion:

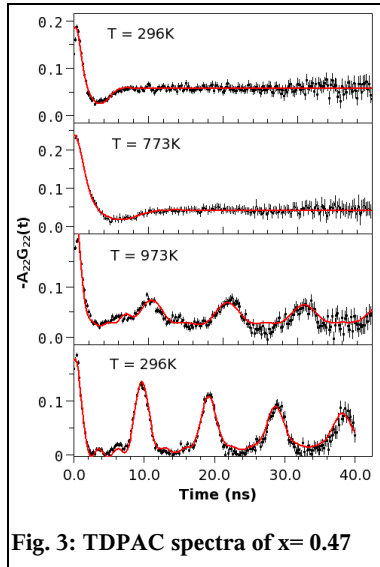The TDPAC measured spectra are shown in Figs. 3-4 (ratios x= 0.47; 0.48, respectively), and the adjusted parameters in Table I. In both cases well defined static interaction frequencies start to show up irreversably around 970 K and 1070 K, respectively. In the x= .47 sample XRD were performed, at RT and after a second heating at 1070 K, on the as prepared sample[**] with both spectra showing quite similar patterns (Figs. 5-6). These XRD results are quite intriguing when compared to the TDPAC x= .47 spectra measured at RT and above 970 K, which look quite different; it would be possible to argue that an XRD characterization (more relate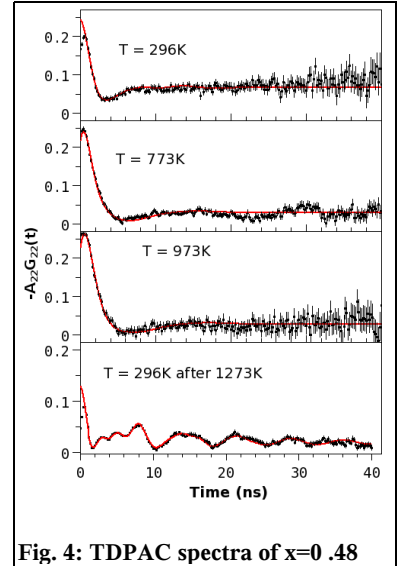d to the bulk structure) may certainly differ from a TDPAC one (more related to the HI occurring in limited circumscribed areas in the sample lattice). Taking into account that samples were prepared in different ways, a previous first TDPAC experiment on the x= 0.48 case showed very similar spectra when compared to our results on x= 0.47, and the discussion of the results was strongly based on lattice vacancies defects, until the PZT decomposition at 1323 K[(14)]; approach well corroborated by the well known fact that, starting around 650 K, both PZT ratios have cubic lattices and, therefore, the EFG's must be zero unless the occurrence of lattice imperfections and/or some other unknown structural reason(s): Figs. 3-4 by no means, at any temperature, display EFG's zero patterns (in this case the anisotropies should have appeared unperturbed).
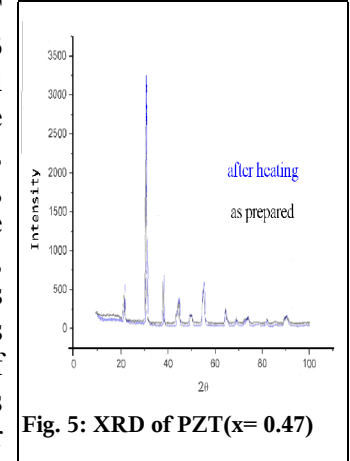
By other side, even still being highly speculative, the TDPAC spectra in the range RT-900 K, with their high frequency distributions rates, may be displaying the coexistence of the monoclinic + tetragonal phases, as recently suggested[(11)] and pointed out in the "Introduction" above. Finally, new TDPAC experiments on PZT (x= 0.47; 0.48), in closer temperature differences, are being performed in order to clear-up this point.

Fig. 3: TDPAC spectra of x= 0.47

Fig. 4: TDPAC spectra of x=0 .48

Fig. 5: XRD of PZT(x= 0.47)

Table I: TDPAC Adjusted Parameters for PZT

x= 0.47

T (K)		f	ν_Q (MHz)	η	δ	λ (MHz)
RT		1	827(9.2)	0	.47(.01)	
773		1	407(9.1)	0	.59(.012)	
973		1	638(3.3)	.15(.02)	.13	
RT (after 1073)		1	701(1.2)	0	.068(.003)	

x=0 .48

T (K)		f	ν_Q (MHz)	η	δ	λ (MHz)
RT	s1	.43	536(60)	.031	.82(.12)	
	s2	.57	760(57)	.44(.07)	.55(.19)	
773	s1	.504	359(14)	.4(.05)	1	
	s2	.496	1100	.5	1	
973	s1	.52	320(13)	.47(.07)	1	
	s2	.48(.1)	920	.4	1	155
RT (after 1273)	s1	.47	921(3)	0	.1(.01)	
	s2	.53	1265(8)	.09(.01)	.09(.01)	90(10)

[**]   see item 3.1

References

1) "Piezoelectric Ceramic" - B. Jaffe, W.R. Cook, H. Jaffe; Academic Press/1971.
2) "Ferroelectric Crystals" - F. Jona, G. Shirane; Dover Publications/1993.
3) G. Shirane et al.; J. Phys. Soc. Japan 7(1952)12.
4) P. Ari-Gur et al.; J. Phys. D Appl. Phys. 8(1975)1856.
5) S.K. Mishra et al.; Appl. Phys. Lett 69(1996)1707.
6) X.H. Du et al.; Appl. Phys. Lett. 72(1998)2421.
7) R. Guo et al.; Phys. Rev. Letters 84(2000)5423
8) A.G. Souza Filho et al.; Phys. Rev. B61(2000)14283.
9) K.C.V. Lima et al.; Phys. Rev. B63(2001)184105.
10) R.S.K. Mishra et al.; Phys. Rev. B64(2001)054101.
11) B. Noheda et al.; Phys. Rev. B63(2001)4103.
12) H. Saitovitch et al.; Química Nova 28/3(2005)529
13) "Nuclear Condensed Matter Physics: Nuclear Methods and Applications" - G. Schatz, A. Weidinger; Wiley&Sons/1992
14) R.E. Alonso et al.; S.S. Communications 107/4(1998)183